

Semantic Communication with Hopfield Memories

Karim Nasreddine*, Christo Kurisummoottil Thomas†, and Walid Saad‡

*Department of Electrical and Computer Engineering, American University of Beirut, Beirut, Lebanon

†Department of Electrical and Computer Engineering, Worcester Polytechnic Institute, Worcester, MA, USA

‡Department of Electrical and Computer Engineering, Virginia Tech, Alexandria, VA, USA

Email: kwn01@aub.edu, cthomas2@wpi.edu, walids@vt.edu

Abstract—Traditional joint source-channel coding employs static learned semantic representations that cannot dynamically adapt to evolving source distributions. Shared semantic memories between transmitter and receiver can potentially enable bandwidth savings by reusing previously transmitted concepts as context to reconstruct data, but require effective mechanisms to determine when current content is similar enough to stored patterns. However, existing hard quantization approaches based on variational autoencoders are limited by frequent memory updates even under small changes in data dynamics, which leads to inefficient usage of bandwidth. To address this challenge, in this paper, a memory-augmented semantic communication framework is proposed where both transmitter and receiver maintain a shared memory of semantic concepts using modern Hopfield networks (MHNs). The proposed framework employs soft attention-based retrieval that smoothly adjusts stored semantic prototype weights as data evolves that enables stable matching decisions under gradual data dynamics. A joint optimization of encoder, decoder, and memory retrieval mechanism is performed with the objective of maximizing a reasoning capacity metric that quantifies semantic efficiency as the product of memory reuse rate and compression ratio. Theoretical analysis establishes the fundamental rate-distortion-reuse tradeoff and proves that soft retrieval reduces unnecessary transmissions compared to hard quantization under bounded semantic drift. Extensive simulations over diverse video scenarios demonstrate that the proposed MHN-based approach achieves substantial bit reductions around 14% on average and up to 70% in scenarios with gradual content changes compared to baseline. Moreover, the simulation results show that the proposed solution achieves a superior performance under transmission errors where baseline hard quantization methods fail abruptly.

I. INTRODUCTION

Traditional source coding techniques [1], even those based on artificial intelligence (AI) [2] typically transmit data representations tightly coupled to pixel-level fidelity for images, videos and word-level fidelity for text, thereby requiring substantial bandwidth even when the receiver is interested in only high-level semantic content. *Semantic communication (SC)* [3]–[6] offers a fundamentally different paradigm by faithfully representing the meaning of the data by encoding the semantics into low-dimensional latent representations that preserve task-relevant information. A learned decoder at the receiver then reconstructs the original content from these compact semantic features [7], [8]. In SC, the transmitter and receiver can share a semantic knowledge base which allows them to reconstruct the content using its local knowledge. This approach leverages advanced AI capabilities at the receiver to minimize over-the-air payload and achieve bandwidth efficiency beyond traditional joint source-channel coding (JSCC). However, such contextual knowledge-based SC faces practical challenges such as (a) *scalability*, as the number of stored semantic concepts grows

with content diversity, (b) need for *efficient knowledge retrieval and update mechanisms* that can adapt to dynamic changes in data while balancing bandwidth efficiency and reconstruction quality, and (c) guarantees of *semantic consistency* between transmitter and receiver knowledge bases under transmission and memory errors.

A. Related works

A number of recent works [9]–[11] explored context-based and memory-augmented SC [9]–[11]. The work in [9] introduced the concept of semantic memory for communication systems, but focused primarily on transformer-based architectures without analyzing the fundamental tradeoffs between memory size, retrieval mechanisms, and communication cost. In [10], the authors proposed emergent semantic languages through signaling games, establishing shared knowledge bases between communicating agents. The work in [12] proposed a knowledge base-assisted SC framework where graph neural networks (GNNs) are used to embed the stored relations among semantic concepts. Recent works like [13] and [14] leverage vector quantized variational autoencoders (VQ-VAE) [15] to learn discrete semantic codebooks for compact indexing and transmission, demonstrating significant compression gains over traditional deep JSCC. While these approaches demonstrate the potential of shared context in enhancing bandwidth efficiency, they face critical limitations. For instance, GNN inference for large-scale knowledge graphs incurs prohibitive latency, while the need for building comprehensive semantic knowledge graphs requires extensive domain-specific ontologies and manual curation, limiting generalizability to dynamic or novel semantic concepts. Moreover, existing SC methods such as those in [9]–[11] do not account for knowledge base mismatches between transmitter and receiver, necessitating efficient memory retrieval and storage mechanisms.

B. Contributions

The main contribution of this paper is to address the aforementioned challenges by proposing a novel memory-augmented SC framework that leverages modern Hopfield networks (MHNs) [16] as shared associative memories. Associative memories use similarity-based retrieval rather than exact matching, providing robust recall under gradual data changes and transmission errors without domain-specific ontologies. Their soft attention mechanism scales efficiently as the number of semantic concepts increases. Although Hopfield networks have been successfully applied to perception and reasoning tasks, their potential for wireless communication systems, particularly for managing the semantic knowledge bases

under bandwidth constraints and channel impairments remains unexplored. In summary, our key contributions are:

- We develop a novel SC framework that integrates a shared associative memory using MHNs into the encoder–decoder system.
- We introduce a new reasoning capacity metric (inspired from [3]) that quantifies semantic communication efficiency as “useful queries per bit.” This metric connects memory reuse to an intelligence-per-bit measure and allows evaluation of how effectively the system converts transmitted bits into correct semantic retrievals.
- We provide a novel theoretical analysis characterizing the rate–distortion–reuse tradeoff. We derive conditions under which the Hopfield associative recall mechanism outperforms VQ’s hard quantization, particularly near decision boundaries where small semantic drifts would cause VQ codebooks to proliferate.
- Extensive simulations conducted over diverse data characteristics demonstrate that MHN-driven SC achieves approximately 14% reduction in average bits per frame compared to VQ at matched reconstruction quality (PSNR within ± 0.2 dB). Under dynamic scenarios, MHNs achieves 70% bit savings (68.7 bits/frame vs. 228.5 bits/frame) by maintaining sustained reuse through gradual content changes, while baseline methods trigger frequent unnecessary refreshes.

II. SYSTEM MODEL

We consider a point-to-point SC system consisting of a transmitter (Tx) and a receiver (Rx) connected over a wireless channel. The Tx aims to communicate a video sequence $\{\mathbf{x}_t\}_{t=1}^T$ to the Rx, where t indexes the frame number and each frame $\mathbf{x}_t \in \mathbb{R}^{H \times W \times 3}$ represents an RGB image of height H and width W . The system objective is to minimize the average bits per frame while ensuring that the Rx’s reconstruction $\hat{\mathbf{x}}_t$ satisfies a target distortion constraint $\mathbb{E}[D(\mathbf{x}_t, \hat{\mathbf{x}}_t)] \leq D_0$, where $D(\cdot, \cdot)$ is a perceptual distortion metric (e.g., mean squared error or structural similarity).

A. Encoder-decoder architecture

A learned encoder $f_\theta : \mathbb{R}^{H \times W \times 3} \rightarrow \mathbb{S}^{d-1}$ maps each frame to a d -dimensional unit-norm latent vector $\mathbf{z}_t = f_\theta(\mathbf{x}_t)$, where $\mathbb{S}^{d-1} = \{\mathbf{z} \in \mathbb{R}^d : \|\mathbf{z}\|_2 = 1\}$ is the $(d-1)$ -dimensional unit sphere and θ are the encoder parameters. A decoder $g_\phi : \mathbb{S}^{d-1} \rightarrow \mathbb{R}^{H \times W \times 3}$ reconstructs frames as $\hat{\mathbf{x}}_t = g_\phi(\hat{\mathbf{z}}_t)$ from the received latent representation $\hat{\mathbf{z}}_t$, where ϕ are the decoder parameters. The spherical latent space enables similarity-based retrieval via cosine similarity $\langle \mathbf{z}_i, \mathbf{z}_j \rangle$.

The *shared associative memory* at time t is a set of M prototype vectors $\mathcal{M}_t = \{\boldsymbol{\mu}_1, \dots, \boldsymbol{\mu}_{M_t}\}$, $\boldsymbol{\mu}_j \in \mathbb{S}^{d-1}$, where each prototype $\boldsymbol{\mu}_j$ represents a learned semantic concept, i.e., a recurring pattern in the latent space corresponding to perceptually similar content such as “blue sky,” “person walking,” or “static background.” Both Tx and Rx maintain identical copies of \mathcal{M}_t , which can be synchronized through the emergent language protocol discussed in [10]. The memory grows dynamically as new semantic concepts are encountered,

up to a maximum capacity M_{\max} . Prototypes can be learned through prior offline training on representative video data or emerge online through the adaptive protocol in [10].

B. Transmission decision

Given the current latent \mathbf{z}_t , the Tx queries the memory \mathcal{M}_{t-1} by computing cosine similarities to all stored prototypes: $s_j = \langle \mathbf{z}_t, \boldsymbol{\mu}_j \rangle$, $j \in [M_{t-1}]$, and identifies the best-matching prototype $j^* = \arg \max_{j \in [M_{t-1}]} s_j$ with maximum similarity $s_{\max} = s_{j^*}$. Using a similarity threshold $\tau \in (0, 1)$, the Tx makes a binary reuse decision:

$$H_t = \begin{cases} 1, & \text{if } s_{\max} \geq \tau \quad (\text{hit: reuse stored prototype}); \\ 0, & \text{if } s_{\max} < \tau \quad (\text{miss: transmit new latent}). \end{cases} \quad (1)$$

The transmission decision can be formalized as a policy $\pi : \mathbb{S}^{d-1} \times \mathcal{M}_{t-1} \rightarrow \{0, 1\} \times [M_{t-1}]$ that maps the query–memory pair $(\mathbf{z}_t, \mathcal{M}_{t-1})$ to a hit/miss indicator H_t and, if $H_t = 1$, the index $j^* \in [M_{t-1}]$ to transmit. On a miss ($H_t = 0$), the policy transmits the new latent \mathbf{z}_t and may append it to memory as $\mathcal{M}_t = \mathcal{M}_{t-1} \cup \{\mathbf{z}_t\}$ if capacity permits ($M_{t-1} < M_{\max}$); otherwise, the memory remains unchanged ($\mathcal{M}_t = \mathcal{M}_{t-1}$).

The Rx reconstructs the latent as:

$$\hat{\mathbf{z}}_t = \begin{cases} \boldsymbol{\mu}_{j^*}, & \text{if } H_t = 1 \quad (\text{retrieve from memory}); \\ Q(\mathbf{z}_t) + \boldsymbol{\epsilon}_t, & \text{if } H_t = 0 \quad (\text{decode transmitted latent}), \end{cases} \quad (2)$$

where $Q(\cdot) : \mathbb{S}^{d-1} \rightarrow \mathbb{S}^{d-1}$ is a quantizer (e.g., uniform scalar quantization with 8 bits per dimension followed by normalization), $\boldsymbol{\epsilon}_t \in \mathbb{R}^d$ is an optional residual for quality enhancement (typically $\boldsymbol{\epsilon}_t = 0$ in our experiments), and $\boldsymbol{\mu}_{j^*} \in \mathcal{M}_{t-1}$ is the retrieved prototype. The Rx then reconstructs the frame as $\hat{\mathbf{x}}_t = g_\phi(\hat{\mathbf{z}}_t)$. The threshold τ controls the rate–distortion–reuse tradeoff: higher τ yields fewer hits (more new transmissions, higher rate, potentially lower distortion), while lower τ increases reuse (more index transmissions, lower rate) but accepts less similar matches that may require residual bits $\boldsymbol{\epsilon}_t$ to maintain reconstruction quality.

C. Communication overhead

We now establish the bit cost model that quantifies the communication overhead for each transmission decision. Let $b_{\text{id}}(M_t) = \lceil \log_2 M_t \rceil$ be the index cost that captures the number of bits required to reference one of M_t prototypes in the shared memory. Let $b_{\text{new}} = 8d$ (under 8 bit quantization) be the cost to transmit a new d -dimensional latent representation. The semantic bits transmitted for frame t are:

$$b_t = H_t \cdot b_{\text{id}}(M_{t-1}) + (1 - H_t) \cdot b_{\text{new}} + b_{\text{res},t}, \quad (3)$$

where the first term accounts for index transmission on a hit ($H_t = 1$), the second term accounts for new latent transmission on a miss ($H_t = 0$), and $b_{\text{res},t} \geq 0$ represents optional residual bits used to encode the error $\boldsymbol{\epsilon}_t$ when quality enhancement is needed to meet a distortion target. In a typical operation, $b_{\text{res},t} = 0$ as the prototype or quantized latent alone suffices for reconstruction within the target quality. The total SC cost over the video sequence is $B_{\text{sem}} = \sum_{t=1}^T b_t$, and the average bits per frame is $\bar{B}_{\text{sem}} = B_{\text{sem}}/T$. The hit rate $\bar{H} = \frac{1}{T} \sum_{t=1}^T H_t$ measures the fraction of frames that successfully reuse stored prototypes.

For comparison, a conventional JSCC method would require B_{raw} bits to transmit the same video at equivalent quality, defining the compression ratio $\gamma = B_{\text{raw}}/B_{\text{sem}}$.

For MHN-driven SC, our objective is to jointly optimize encoder f_θ and decoder g_ϕ to produce semantically meaningful latent representations enabling effective context reuse while maintaining reconstruction quality and robustness to transmission errors. The optimal threshold τ^* must balance the rate-distortion-reuse tradeoff, where higher τ reduces memory hits (higher rate) but ensures better matches (lower distortion), while lower τ increases reuse (lower rate) but accepts poorer matches. We now formulate the optimization problem.

III. PROPOSED ASSOCIATIVE MEMORY BASED SC

We propose MHNs as the shared associative memory because their soft retrieval mechanism allows stable matches near threshold τ , provides robustness through weighted prototype combinations, and minimizes storage by preventing duplicates.

A. Modern Hopfield network memory

For a given query, i.e., the latent vector \mathbf{z}_t and stored prototypes $\{\boldsymbol{\mu}_j\}_{j=1}^{M_t}$, the Hopfield memory computes semantic similarity-weighted activations: $w_j = \frac{\exp(\beta \langle \mathbf{z}_t, \boldsymbol{\mu}_j \rangle)}{\sum_{k=1}^{M_t} \exp(\beta \langle \mathbf{z}_t, \boldsymbol{\mu}_k \rangle)}$, and returns a normalized latent vector:

$$\tilde{\mathbf{z}}_t = \frac{\sum_{j=1}^{M_t} w_j \boldsymbol{\mu}_j}{\left\| \sum_{j=1}^{M_t} w_j \boldsymbol{\mu}_j \right\|_2}, \quad (4)$$

where $\beta > 0$ controls retrieval sharpness. As $\beta \rightarrow \infty$, the weights concentrate on a single prototype ($w_{j^*} \rightarrow 1$), recovering hard nearest-neighbor selection, while lower β produces smooth blending across distinct semantic concepts.

Next, we introduce a *reasoning capacity metric* that measures semantic efficiency, i.e. how effectively a context aware SC converts transmitted bits into useful semantic information.

B. Reasoning capacity metric

We define the *semantic efficiency* as $\eta = \underbrace{\frac{Q}{T}}_{\text{hit rate}} \times \underbrace{\frac{B_{\text{raw}}}{B_{\text{sem}}}}_{\text{compression ratio}}$,

where $H_t \in \{0, 1\}$ is the hit indicator at time t , $Q \triangleq \sum_{t=1}^T H_t$ is the total number of hits over a sequence of length T , B_{raw} is the number of bits required by a non-semantic (raw) codec, and B_{sem} is the number of bits transmitted by the semantic system. This metric quantifies the system's ability to reuse semantic content (Q/T) while achieving bandwidth savings ($B_{\text{raw}}/B_{\text{sem}}$). Following [3], the corresponding *reasoning capacity* can be written as:

$$C_R = \Omega \log_2(1 + \eta), \quad (5)$$

where $\Omega > 0$ is a scaling constant (typically $\Omega = 1$ for dimensionless capacity, or chosen to map to physical units like bits/s/Hz). The logarithmic form ensures: (i) C_R grows approximately linearly for small η ($C_R \approx \Omega \eta / \ln 2$ when $\eta \ll 1$), capturing incremental improvements; and (ii) C_R saturates for large η , avoiding unbounded values as compression approaches the theoretical limit. A high reasoning capacity implies that the system successfully retrieves stored semantics (high Q/T) while minimizing transmission overhead (high $B_{\text{raw}}/B_{\text{sem}}$). Memory architectures that reduce unnecessary

New transmissions near threshold τ increase Q/T , directly improving C_R . We define $D(\hat{\mathbf{x}}_t, \mathbf{x}_t)$ as a distortion metric (e.g., MSE), with $\bar{D} = \frac{1}{T} \sum_{t=1}^T D(\hat{\mathbf{x}}_t, \mathbf{x}_t)$ being the average distortion. The SC design objective is to maximize reasoning capacity subject to a reconstruction quality constraint.

C. Problem formulation

We formulate the MHN-driven SC system design as the following constrained optimization problem:

$$\max_{\theta, \phi, \tau, \{b_{\text{res}, t}\}_{t=1}^T} C_R(\theta, \phi, \tau) \quad (6)$$

$$\text{s.t. } \bar{D}(\theta, \phi, \pi_\tau) \leq D_0, \quad (6a)$$

$$H_t = \mathbf{1}\{\langle \mathbf{z}_t, \boldsymbol{\mu}_j^* \rangle \geq \tau\}, \quad \forall t \in [T], \quad (6b)$$

$$z_t = f_\theta(x_t), \quad \|z_t\|_2 = 1, \quad \forall t, \quad (6c)$$

$$\hat{\mathbf{x}}_t = g_\phi(\hat{\mathbf{z}}_t), \quad \forall t, \quad b_{\text{res}, t} \geq 0, \quad \forall t, \quad (6d)$$

$$M_t \leq M_{\text{max}}, \quad \forall t. \quad (6e)$$

The objective in (6) maximizes the reasoning capacity. (6a) enforces a target reconstruction quality D_0 , while (6b) defines the hit/miss logic via threshold τ . The remaining constraints (6c)-(6e) capture the encoder-decoder-memory dynamics and bit allocations. Note that θ and ϕ affect both the latent space geometry (hit/miss decisions) and reconstruction quality (D_0). Jointly optimizing (θ, ϕ, τ) requires gradient-based training with differentiable relaxations of H_t (e.g., straight-through estimators or Gumbel-softmax). For tractability, we reformulate the constrained problem as an unconstrained Lagrangian:

$$\mathcal{L}(\theta, \phi, \tau; \lambda) = \frac{1}{T} B_{\text{sem}}(\theta, \phi, \pi_\tau) + \lambda (\bar{D}(\theta, \phi, \pi_\tau) - D_0), \quad (7)$$

where $\lambda > 0$ is a multiplier for the distortion constraint. We then seek to maximize \mathcal{L} over (θ, ϕ, τ) .

D. Solution approach

We solve (7) using alternating gradient-based optimization: In step 1, we replace the hard indicator $H_t = \mathbf{1}\{\langle \mathbf{z}_t, \boldsymbol{\mu}_j^* \rangle \geq \tau\}$ with a smooth approximation $\bar{H}_t = \sigma(\alpha(\langle \mathbf{z}_t, \boldsymbol{\mu}_j^* \rangle - \tau))$, where $\sigma(\cdot)$ is the sigmoid function and $\alpha > 0$ controls sharpness (higher α approaches the hard threshold). This enables backpropagation through the hit/miss decision. In step 2, for fixed λ , encoder-decoder parameters are updated via:

$$\theta \leftarrow \theta - \eta_\theta \nabla_\theta \mathcal{L}(\theta, \phi, \tau; \lambda), \quad \phi \leftarrow \phi - \eta_\phi \nabla_\phi \mathcal{L}(\theta, \phi, \tau; \lambda),$$

where $\eta_\theta, \eta_\phi > 0$ are learning rates. The threshold τ is updated similarly or via grid search over $[0, 1]$ for each (θ, ϕ) . Finally, λ is adjusted to enforce the constraint:

$$\lambda \leftarrow \max(0, \lambda + \eta_\lambda (\bar{D}(\theta, \phi, \tau) - D_0)), \quad (8)$$

where $\eta_\lambda > 0$ is the step size. If $\bar{D} > D_0$ (quality violation), λ increases to penalize distortion more heavily. This procedure alternates between minimizing \mathcal{L} over (θ, ϕ, τ) and updating λ until convergence to a saddle point satisfying the quality constraint. The details of the solution is outlined in Algorithm 1.

E. Theoretical analysis

Theorem 1 (Rate-Distortion-Reuse Tradeoff). *For fixed encoder-decoder (θ, ϕ) , the triple (C_R, \bar{D}, τ) lies on a Pareto frontier $\mathcal{F} = \{(C_R(\theta, \pi, \tau), \bar{D}(\theta, \pi, \tau), \tau) : \tau \in (0, 1)\}$, characterized by:*

- 1) Monotonic relationships: $\frac{\partial C_R}{\partial \tau} < 0, \frac{\partial \bar{D}}{\partial \tau} < 0, \frac{\partial \bar{H}}{\partial \tau} < 0$.

2) Optimal threshold: For a target distortion D_0 , the optimal reuse threshold is

$$\tau^*(D_0) = \inf\{\tau \in (0, 1) : \bar{D}(\tau) \leq D_0\}, \quad (9)$$

and $\tau^*(D_0)$ is non-increasing in D_0 .

3) Pareto optimality: If we consider two operating points $(\tau_1, D_1, C_{R,1})$ and $(\tau_2, D_2, C_{R,2})$ on \mathcal{F} , then it is not possible for one to dominate the other in both distortion and capacity. Specifically, there is no $(\tau_1, D_1, C_{R,1})$ and $(\tau_2, D_2, C_{R,2})$ on \mathcal{F} such that $D_1 \leq D_2$ and $C_{R,1} \geq C_{R,2}$ with at least one strict inequality.

Proof: The proof is omitted due to space constraints. ■

Theorem 1 establishes that all memory architectures face the same fundamental constraints. However, the *shape and position* of the Pareto frontier depends critically on the retrieval mechanism. We now formalize when MHN’s associative recall provides a quantifiable advantage over VQ’s hard quantization.

Theorem 2. [MHN Bit Savings] Consider a video sequence where latents exhibit bounded semantic drift around a stored prototype $z_t = \mu^* + \delta_t$, where $\|\delta_t\|_2 \leq \varepsilon$ for some $\mu^* \in \mathcal{M}$ and small $\varepsilon > 0$. Assume all prototypes are unit-norm and lie on the sphere \mathbb{S}^{d-1} . For a given threshold $\tau \in (0, 1)$ and Hopfield inverse temperature $\beta > 0$, let N_{refresh}^H and N_{refresh}^V denote the number of memory refresh events (new transmissions) for Hopfield and VQ respectively over a horizon of T frames. Under the following conditions:

- 1) The prototypes $\{\mu_j\}_{j=1}^M$ satisfy minimum separation: $\min_{j \neq j'} \|\mu_j - \mu_{j'}\|_2 \geq \Delta > 0$.
- 2) The drift δ_t is i.i.d. with $\mathbb{E}[\delta_t] = 0$ and $\mathbb{E}[\|\delta_t\|_2^2] = \sigma^2 \leq \varepsilon^2$.
- 3) The threshold satisfies $\tau < 1 - \varepsilon - \frac{\varepsilon^2}{2}$ (boundary regime).

Then, number of memory updates for MHN-driven SC is lower than that of VQ-VAE and is bounded as:

$$\mathbb{E}[N_{\text{refresh}}^H] \leq \mathbb{E}[N_{\text{refresh}}^V] \cdot \left(1 - \frac{\beta\varepsilon^2}{2d}\right) + O(\varepsilon^3) \quad (10)$$

where the expectation is over the drift realizations $\{\delta_t\}_{t=1}^T$.

Proof: See Appendix A. ■

Corollary 1. Under the conditions of Theorem 2, the expected semantic bit savings are:

$$\mathbb{E}[B_{\text{sem}}^V - B_{\text{sem}}^H] \geq (b_{\text{new}} - \overline{\log_2 M}) \cdot \frac{\beta\varepsilon^2 T}{2d} \mathbb{E}[N_{\text{refresh}}^V]. \quad (11)$$

Proof: See Appendix B. ■

IV. SIMULATION RESULTS AND ANALYSIS

We evaluate the proposed SC system on a variety of video content types and compare it against a VQ-VAE based SC [13], [14] baseline. We implement a lightweight learned encoder-decoder (e.g., a β -VAE [17] or a shallow CNN autoencoder) that produces d -dimensional latent vectors z_t , normalized to unit norm. Unless otherwise specified, new latent vectors are quantized with 8 bits per value (i.e., $b_{\text{new}} = 8d$). All comparisons between Hopfield and VQ memories are conducted under matched reconstruction fidelity: we calibrate the similarity threshold τ for each method such that the peak signal-to-noise ratio (PSNR) of the reconstructed video falls within a ± 0.2 dB range for both methods.

Algorithm 1 Training Procedure for Memory-Based SC

```

Require: Training video data  $\{\mathbf{x}_t\}_{t=1}^T$ , target distortion  $D_0$ 
Ensure: Encoder  $f_\theta$ , decoder  $g_\phi$ , threshold  $\tau$ 
1: Initialize  $\theta, \phi$  randomly,  $\tau = 0.7$ ,  $\lambda = 1.0$ 
2: Initialize memory  $\mathcal{M}_0 = \emptyset$ 
3: for epoch = 1 to  $N_{\text{epochs}}$  do
4:   for batch  $\{\mathbf{x}_t\}_{t=1}^B$  do
5:     Encode:  $\mathbf{z}_t = f_\theta(\mathbf{x}_t) / \|f_\theta(\mathbf{x}_t)\|_2$ 
6:     Compute hits:  $\hat{H}_t = \sigma(\alpha(\langle \mathbf{z}_t, \mu_j^* \rangle - \tau))$ 
7:     Retrieve/transmit:  $\hat{\mathbf{z}}_t$  via Eq. (2)
8:     Decode:  $\hat{\mathbf{x}}_t = g_\phi(\hat{\mathbf{z}}_t)$ 
9:     Compute  $\mathcal{L}(\theta, \phi, \tau; \lambda)$  via Eq. (7)
10:    Update:  $\theta \leftarrow \theta - \eta_\theta \nabla_\theta \mathcal{L}$ 
11:    Update:  $\phi \leftarrow \phi - \eta_\phi \nabla_\phi \mathcal{L}$ 
12:    Update:  $\tau \leftarrow \tau - \eta_\tau \nabla_\tau \mathcal{L}$  (or grid search)
13:    Update memory:  $\mathcal{M} \leftarrow \mathcal{M} \cup \{\mathbf{z}_t : H_t = 0\}$ 
14:  end for
15:  Update multiplier:  $\lambda \leftarrow \max(0, \lambda + \eta_\lambda(\bar{D} - D_0))$ 
16: end for
17: return  $f_\theta, g_\phi, \tau$ 

```

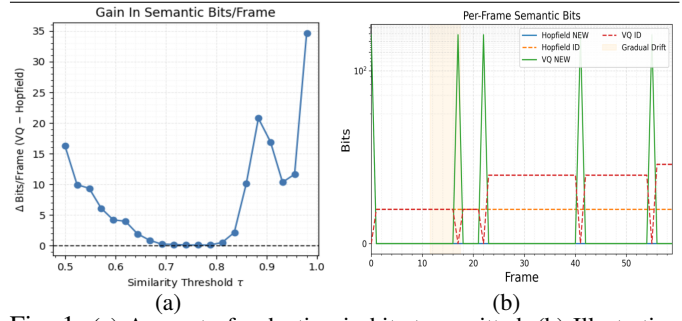


Fig. 1: (a) Amount of reduction in bits transmitted. (b) Illustration of new latent vector transmissions for VQ-VAE compared to stable knowledge base for MHN.

A. Dataset description

We use synthetic and real video clips from the imageio library [18] across eight content regimes: *static*, *low_motion*, *high_motion*, *scene_change*, *repetitive_return*, *cam_shake*, *high_texture*, and *illum_change*, with $T \in [36, 80]$ frames. We test three scenarios: (A) *STABLE*, where frames remain highly similar over time (*static*, *low_motion*, *repetitive_return*); (B) *GRADUAL DRIFT*, where changes accumulate slowly from lighting, camera motion, or appearance variations (*illum_change*, minor *cam_shake*); and (C) *MODERATE*, with intermediate dynamics between stable and drifting content (*high_motion*, *high_texture*). We evaluate performance by varying threshold τ , memory size M_{max} , and robustness to memory corruption.

B. Bandwidth savings

Table I shows the bits per frame and reasoning capacity for three scenarios. In the *STABLE* and *MODERATE* scenarios, MHN and VQ-VAE perform equivalently, with 9.51 bits/frame, hit rate 0.978, and $C_R = 14.26$. In the *GRADUAL DRIFT* scenario (slow concept shift), MHN transmits about 70% fewer bits per frame than VQ-VAE (68.66 vs. 228.53) while maintaining a higher hit rate (0.825 vs. 0.408) and stronger compression ($C_R = 14.26$ vs. 9.04). Fig. 1a shows the gain in the average amount of bits communicated for MHN-driven SC compared to VQ-VAE baseline for varying similarity threshold τ . Clearly, our MHN approach outperforms VQ-VAE when there is a gradual change in semantics across the frames. Fig. 1b shows that VQ-VAE baseline requires frequent updates to the knowledge base, which are illustrated by the spikes

TABLE I: Bits/frame for diverse content types.

Protocol	Method	Bits/frame	Hit rate	C_R
STABLE	Hopfield	9.51	0.978	14.26
	VQ	9.51	0.978	14.26
GRADUAL DRIFT	Hopfield	68.66	0.825	14.26
	VQ	228.53	0.408	9.04
MODERATE	Hopfield	9.51	0.978	14.26
	VQ	9.51	0.978	14.26

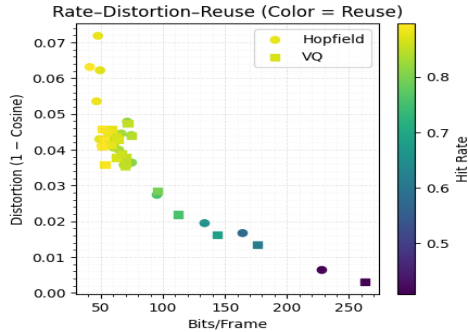


Fig. 2: Rate-distortion-reuse tradeoff. corresponding to new latent vector transmissions (see legends "VQ NEW" vs "Hopfield NEW").

C. Reuse vs. diversity tradeoff

Fig. 2 shows that Hopfield networks consistently achieve lower transmission rates (bits/frame) than VQ at comparable distortion levels; the advantage increases as the hit rate decreases, reaching up to $\sim 15\text{--}25\%$ bit savings in the low-hit-rate regime. (dark blue points). The soft associative retrieval in Hopfield allows better interpolation between stored prototypes, reducing the need to transmit new representations compared to VQ's hard selection. This demonstrates that Hopfield's continuous retrieval mechanism provides a tangible rate-distortion advantage for SC in video streaming scenarios.

D. Robustness to Rx memory errors

We evaluate robustness under two Rx memory corruption modes: (a) ID-map de-synchronization, where the mapping from semantic IDs to memory slots is randomly permuted for fraction p of entries, and (b) vector perturbation, where stored prototypes are corrupted by additive Gaussian noise $\epsilon_j \sim \mathcal{N}(0, \sigma^2 \mathbf{I})$ and re-normalized. The Rx verifies each ID transmission using a short cue (SimHash fingerprint of $B_{\text{cue}} = 32$ bits, tolerating up to 25% bit errors) and performs content-addressable lookup on cue f , requesting a refresh if verification still fails. Figures 3a and 3b show that Hopfield's associative retrieval offers a semantic robustness advantage in the regime of mild memory corruption ($p \leq 0.1, \sigma \leq 0.05$), incurring fewer refreshes than VQ's hard nearest-centroid lookup and thus saving bits for example, achieving $\Delta\text{bits} = +381$ at $p = 0$ versus -381 at $p = 0.5$, demonstrating that soft attractor dynamics tolerate small misalignments better than hard quantization near decision boundaries. However, under severe corruption ($\sigma \geq 0.10$), the Hopfield attractor can be misled by averaging corrupted neighbors, causing the advantage to narrow or reverse, highlighting a tradeoff between semantic tolerance and robustness that can be tuned via cue length, association sharpness β , and similarity threshold τ .

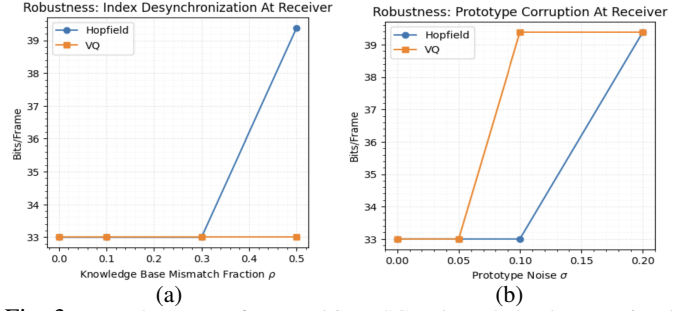


Fig. 3: (a) Robustness of MHN-driven SC to knowledge base retrieval mechanism errors, and (b) stored prototype mismatches.

V. CONCLUSION

In this paper, we have presented a memory-augmented SC framework leveraging MHNs as shared associative memories between Tx and Rx. The proposed soft attention-based retrieval mechanism maintains stable matching decisions under gradual semantic drift, avoiding the bandwidth waste caused by baseline methods' hard quantization approach. We introduced a reasoning capacity metric that quantifies semantic efficiency as the product of memory reuse rate and compression ratio. Theoretical analysis established the fundamental rate-distortion-reuse tradeoff and proved that soft retrieval reduces unnecessary transmissions compared to hard quantization under bounded semantic drift conditions. Extensive simulations demonstrated that the MHN-based approach achieves approximately 14% average bit reduction across diverse video scenarios and up to 70% savings under gradual content changes, while maintaining reconstruction quality and exhibiting graceful degradation under transmission errors.

REFERENCES

- [1] T. M. Cover and J. A. Thomas, *Elements of Information Theory*, John Wiley & Sons, 1991.
- [2] N. Farsad, M. Rao, and A. Goldsmith, "Deep learning for joint source-channel coding of text," in *2018 IEEE International Conference on Acoustics, Speech and Signal Processing (ICASSP)*, Apr. 2018.
- [3] C. Chaccour, W. Saad, M. Debbah, Z. Han, and H. V. Poor, "Less data, more knowledge: Building next-generation semantic communication networks," *IEEE Communications Surveys & Tutorials*, vol. 27, no. 1, pp. 37–76, 2024.
- [4] Q. Lan, D. Wen, Z. Zhang, Q. Zeng, X. Chen, P. Popovski, and K. Huang, "What is semantic communication? a view on conveying meaning in the era of machine intelligence," *Journal of Communications and Information Networks*, vol. 6, no. 4, pp. 336–371, 2021.
- [5] E. C. Strinati and S. Barbarossa, "6g networks: Beyond shannon towards semantic and goal-oriented communications," *Computer Networks*, vol. 190, pp. 107930, 2021.
- [6] Marios Kountouris and Nikolaos Pappas, "Semantics-empowered communication for networked intelligent systems," *IEEE Communications Magazine*, vol. 59, no. 6, pp. 96–102, 2021.
- [7] E. Xie, "Deep learning enabled semantic communication systems," *IEEE Transactions on Signal Processing*, vol. 69, pp. 2663–2678, 2021.
- [8] H. Fu et al., "Vector quantized semantic communication," in *Proceedings of IEEE International Conference on Communications (ICC)*, 2023.
- [9] H. Xie, Z. Qin, and G. Y. Li, "Semantic communication with memory," *IEEE Journal on Selected Areas in Communications*, vol. 41, no. 8, pp. 2658–2669, 2023.
- [10] C. K. Thomas and W. Saad, "Neuro-symbolic causal reasoning meets signaling game for emergent semantic communications," *IEEE Transactions on Wireless Communications*, vol. 23, no. 5, pp. 1–?, May 2024.
- [11] J. Ren, Z. Zhang, J. Xu, G. Chen, Y. Sun, P. Zhang, and S. Cui, "Knowledge base enabled semantic communication: A generative perspective," *arXiv preprint arXiv:2311.12443*, 2023.
- [12] N. Hello, P. Di Lorenzo, and E. C. Strinati, "Semantic communication enhanced by knowledge graph representation learning," in *Proceedings of IEEE 25th International Workshop on Signal Processing Advances in Wireless Communications (SPAWC)*, September 2024.

- [13] Q. Fu, H. Xie, Z. Qin, G. Slabaugh, and X. Tao, “Vector quantized semantic communication system,” *IEEE Wireless Communications Letters*, vol. 12, no. 6, pp. 982–986, 2023.
- [14] Y. Miao, Z. Li, Y. Wang, D. Hu, J. Yan, and Y. Wang, “Vq-deepvsc: A dual-stage vector quantization framework for video semantic communication,” *arXiv preprint arXiv:2409.03393*, 2024.
- [15] A. van den Oord, O. Vinyals, and K. Kavukcuoglu, “Neural discrete representation learning,” in *Advances in Neural Information Processing Systems (NeurIPS)*, 2017, vol. 30, pp. 6306–6315.
- [16] H. Ramsauer, “Hopfield networks is all you need,” in *Proceedings of International Conference on Machine Learning (ICML)*, 2021.
- [17] D. P. Kingma and M. Welling, “Auto-encoding variational Bayes,” in *Proceedings of International Conference on Learning Representations (ICLR)*, 2014.
- [18] Almar Klein and contributors, “Imageio: Python library for reading and writing image data,” 2023.

APPENDIX A

PROOF OF THEOREM 2

The expected refresh counts are $\mathbb{E}[N_{\text{refresh}}^V] = T \cdot P_{\text{miss}}^V$, $\mathbb{E}[N_{\text{refresh}}^H] = T \cdot P_{\text{miss}}^H$, where $P_{\text{miss}}^V = \mathbb{P}(\text{Miss}_t^V = 1)$ and $P_{\text{miss}}^H = \mathbb{P}(\text{Miss}_t^H = 1)$. Given $z_t = \mu^* + \delta_t$, the similarity to the correct prototype is: $s_t^* = \langle z_t, \mu^* \rangle = \langle \mu^* + \delta_t, \mu^* \rangle = \langle \mu^*, \mu^* \rangle + \langle \delta_t, \mu^* \rangle = 1 + \langle \delta_t, \mu^* \rangle$ (using $\|\mu^*\|_2 = 1$). For $j \neq j^*$, we define $\rho = \max_{j \neq j^*} \langle \mu^*, \mu_j \rangle$. By the minimum separation assumption, we have $\|\mu_j - \mu^*\|_2^2 = 2 - 2\langle \mu_j, \mu^* \rangle \geq \Delta^2$. Therefore, $\langle \mu_j, \mu^* \rangle \leq 1 - \frac{\Delta^2}{2} =: \rho < 1$. Therefore, the similarity to a competing prototype is

$$\langle z_t, \mu_j \rangle = \langle \mu^*, \mu_j \rangle + \langle \delta_t, \mu_j \rangle \leq \rho + \epsilon \quad (12)$$

This follows from Cauchy-Schwarz inequality $|\langle \delta_t, \mu_j \rangle| \leq \|\delta_t\|_2 \|\mu_j\|_2 \leq \epsilon$. Under the assumption that μ^* is the closest prototype (satisfied when ϵ is small relative to prototype separation), the miss condition simplifies to: $1 + \langle \delta_t, \mu^* \rangle < \tau$. Therefore, we obtain $P_{\text{miss}}^V = \mathbb{P}(\langle \delta_t, \mu^* \rangle < \tau - 1)$. We now derive the associative boost that MHN provides through its soft attention mechanism.

1) *Compute soft attention weights:* The attention weight for the correct prototype is:

$$w_{j^*}(\beta) = \frac{\exp(\beta(1 + \langle \delta_t, \mu^* \rangle))}{\exp(\beta(1 + \langle \delta_t, \mu^* \rangle)) + \sum_{j \neq j^*} \exp(\beta \langle z_t, \mu_j \rangle)}. \quad (13)$$

For simplicity, let $\xi = \langle \delta_t, \mu^* \rangle$ and $\xi_j = \langle \delta_t, \mu_j \rangle$ for $j \neq j^*$, and factoring out $\exp(\beta(1 + \xi))$, and defining $\gamma_j = \langle \mu^*, \mu_j \rangle - 1 \leq \rho - 1 < 0$ (since prototypes are separated), (13) becomes

$$w_{j^*}(\beta) = \frac{1}{1 + \sum_{j \neq j^*} \exp(\beta(\gamma_j + \xi_j - \xi))}. \quad (14)$$

For small ϵ , $|\xi|, |\xi_j| \leq \epsilon$, $\gamma_j + \xi_j - \xi \leq (\rho - 1) + 2\epsilon < 0$ (using the boundary assumption), which implies $1 - \rho > 2\epsilon$. Further, performing a Taylor expansion around $\xi = \xi_j = 0$. Let $\alpha = \frac{1}{1 + (M-1) \exp(\beta(\rho-1))}$ be the weight when $\delta_t = 0$. For small ϵ : $w_{j^*}(\beta) \approx \alpha(1 + \beta\xi + O(\epsilon^2))$. Following similar steps, we obtain for competing prototypes,

$$w_j(\beta) \approx \frac{1 - \alpha}{M - 1} (1 - \beta\xi + O(\epsilon^2)) \quad \text{for } j \neq j^*$$

2) *Similarity after MHN Update:* We write $\langle \tilde{z}_t, \mu^* \rangle = \sum_{j=1}^M w_j(\beta) \langle \mu_j, \mu^* \rangle = w_{j^*}(\beta) \cdot 1 + \sum_{j \neq j^*} w_j(\beta) \langle \mu_j, \mu^* \rangle$. Using the approximations derived above, we can write it as:

$$\begin{aligned} \langle \tilde{z}_t, \mu^* \rangle &\approx \alpha(1 + \beta\xi) + (1 - \alpha)(1 - \beta\xi)\rho \\ &= \alpha(1 - \rho) + \rho + \beta\xi[\alpha - (1 - \alpha)\rho] \end{aligned} \quad (15)$$

For large β or well-separated prototypes, $\alpha \approx 1$, so: $\langle \tilde{z}_t, \mu^* \rangle \approx 1 + \beta\xi + O(\epsilon^2)$. Including second-order terms in the Taylor expansion (derived from the exponential in the weights and the normalization):

$$\langle \tilde{z}_t, \mu^* \rangle \approx 1 + \langle \delta_t, \mu^* \rangle + \frac{\beta}{2d} \|\delta_t\|_2^2 + O(\epsilon^3) \quad (16)$$

$\frac{\beta}{2d} \|\delta_t\|_2^2$ arises from the curvature of the exponential softmax, averaging over d dimensions, and is the normalization factor.

Next, we compute the Hopfield miss probability. Hopfield misses when $\langle \tilde{z}_t, \mu^* \rangle < \tau$. Using the boost, $1 + \langle \delta_t, \mu^* \rangle + \frac{\beta}{2d} \|\delta_t\|_2^2 < \tau$. Rearranging gives $\langle \delta_t, \mu^* \rangle < \tau - 1 - \frac{\beta}{2d} \|\delta_t\|_2^2$. Since $\|\delta_t\|_2^2 \geq 0$:

$$P_{\text{miss}}^H = \mathbb{P}\left(\langle \delta_t, \mu^* \rangle < \tau - 1 - \frac{\beta}{2d} \|\delta_t\|_2^2\right). \quad (17)$$

(17) can be bounded as $P_{\text{miss}}^H \leq \mathbb{P}(\langle \delta_t, \mu^* \rangle < \tau - 1) = P_{\text{miss}}^V$. For tighter analysis, use $\|\delta_t\|_2^2 \leq \epsilon^2$, which leads to

$$P_{\text{miss}}^H \leq \mathbb{P}\left(\langle \delta_t, \mu^* \rangle < \tau - 1 - \frac{\beta\epsilon^2}{2d}\right). \quad (18)$$

3) *Ratio of miss probabilities:* The VQ miss probability can be written as $P_{\text{miss}}^V = \int_{-\infty}^{\tau-1} p(\xi) d\xi$. For Hopfield (to first order in ϵ^2), this becomes $P_{\text{miss}}^H \approx \int_{-\infty}^{\tau-1 - \frac{\beta\epsilon^2}{2d}} p(\xi) d\xi$. Further, the difference can be computed as

$$P_{\text{miss}}^V - P_{\text{miss}}^H \approx \int_{\tau-1 - \frac{\beta\epsilon^2}{2d}}^{\tau-1} p(\xi) d\xi \quad (19)$$

For small $\frac{\beta\epsilon^2}{2d}$, (19) can be approximated as $\approx p(\tau-1) \cdot \frac{\beta\epsilon^2}{2d}$. The ratio becomes $\frac{P_{\text{miss}}^H}{P_{\text{miss}}^V} = 1 - \frac{p(\tau-1)}{P_{\text{miss}}^V} \cdot \frac{\beta\epsilon^2}{2d}$. We define $C = \frac{p(\tau-1)}{P_{\text{miss}}^V}$ (a constant depending on the distribution of δ_t and threshold τ). Then $P_{\text{miss}}^H = P_{\text{miss}}^V \left(1 - C \frac{\beta\epsilon^2}{2d}\right) + O(\epsilon^3)$. Since the drift δ_t is i.i.d. across frames, we can write after aggregating over horizon T as: $\mathbb{E}[N_{\text{refresh}}^V] = \sum_{t=1}^T \mathbb{E}[\text{Miss}_t^V] = T \cdot P_{\text{miss}}^V$, and $\mathbb{E}[N_{\text{refresh}}^H] = \sum_{t=1}^T \mathbb{E}[\text{Miss}_t^H] = T \cdot P_{\text{miss}}^H$. Substituting the ratio, we get

$$\mathbb{E}[N_{\text{refresh}}^H] = \mathbb{E}[N_{\text{refresh}}^V] \left(1 - C \frac{\beta\epsilon^2}{2d}\right) + O(\epsilon^3) \quad (20)$$

Absorbing the constant C (which depends on the drift distribution but is $O(1)$):

$$\mathbb{E}[N_{\text{refresh}}^H] \leq \mathbb{E}[N_{\text{refresh}}^V] \cdot \left(1 - \frac{\beta\epsilon^2}{2d}\right) + O(\epsilon^3) \quad (21)$$

This completes the proof of Theorem 2. \square

APPENDIX B

PROOF OF COROLLARY 1(BIT SAVINGS)

Proof. From (3), each refresh (miss) costs b_{new} bits (to send a new latent), while a hit costs $\log_2 M$ bits (to send an index). The difference in semantic bits between VQ and Hopfield is $\mathbb{E}[B_{\text{sem}}^V - B_{\text{sem}}^H] = (b_{\text{new}} - \log_2 M) \cdot \mathbb{E}[N_{\text{refresh}}^V - N_{\text{refresh}}^H]$. From Theorem 2, we have $\mathbb{E}[N_{\text{refresh}}^V - N_{\text{refresh}}^H] = \mathbb{E}[N_{\text{refresh}}^V] \cdot \frac{\beta\epsilon^2}{2d} + O(\epsilon^3)$. Therefore:

$$\mathbb{E}[B_{\text{sem}}^V - B_{\text{sem}}^H] = (b_{\text{new}} - \log_2 M) \cdot \frac{\beta\epsilon^2}{2d} \mathbb{E}[N_{\text{refresh}}^V] + O(\epsilon^3) \quad (22)$$

Dropping higher-order terms yields the stated result. \square